Supplementary Material

Characterization of tioconazole mesylate. Single crystal X-ray diffraction, Hirshfeld surface analysis, stability and DFT-assisted infrared spectral assignment

Aldana B. Moroni,[a,b,§] María Florencia Silveira[a] and Natalia L. Calvo[a,b,*]

[a]Instituto de Química Rosario "Dr. Edmundo A. Rúveda" (IQUIR, CONICET-UNR), Suipacha 531, Rosario S2002LRK, Argentina; [b]Área de Análisis de Medicamentos, Facultad de Ciencias Bioquímicas y Farmacéuticas, Universidad Nacional de Rosario, Suipacha 531, Rosario S2002LRK, Argentina; [§]Present address: Instituto de Investigaciones en Ingeniería Ambiental, Química y Biotecnología Aplicada (INGEBIO), Av. Pellegrini 3314, Rosario S2002QEO, Argentina

Email: calvo@iquir-conicet.gov.ar

Table of Contents

Figure S1. 400 MHz ^{1}H NMR spectrum of TCZ-Ms in DMSO-d_6 ..... S2
Figure S2. 100 MHz ^{13}C NMR spectrum of TCZ-Ms in DMSO-d_6 ..... S2
Figure S3. HSQC spectrum of TCZ-Ms in DMSO-d_6 ..... S3
Figure S4. HMBC spectrum of TCZ-Ms in DMSO-d_6 ..... S3
Figure S5. COSY spectrum of TCZ-Ms in DMSO-d_6 ..... S4
Figure S6. ^{15}N HMBC spectrum of TCZ-Ms in DMSO-d_6 ..... S4
Figure S7. ORTEP representation and atom numbering of TCZ-Ms S5
Table S1-4. Crystallographic tables. Bond lengths, angles, torsions, H-bonds S6
Figure S8. ATR/MIR spectrum of TCZ-Ms. Wavenumber range 400-4000 cm^{-1} S11
Figure S9. Correlation between observed and calculated vibrational frequencies of TCZ-Ms in the MIR region S12
Table S5. Experimental ATR/MIR spectra of TCZ and TCZ-Ms; calculated bands for TCZ-Ms and their corresponding assignments S13
Table S6. Stability. Main characteristics of the heating/cooling cycles S14
References S15

 ©AUTHOR(S)

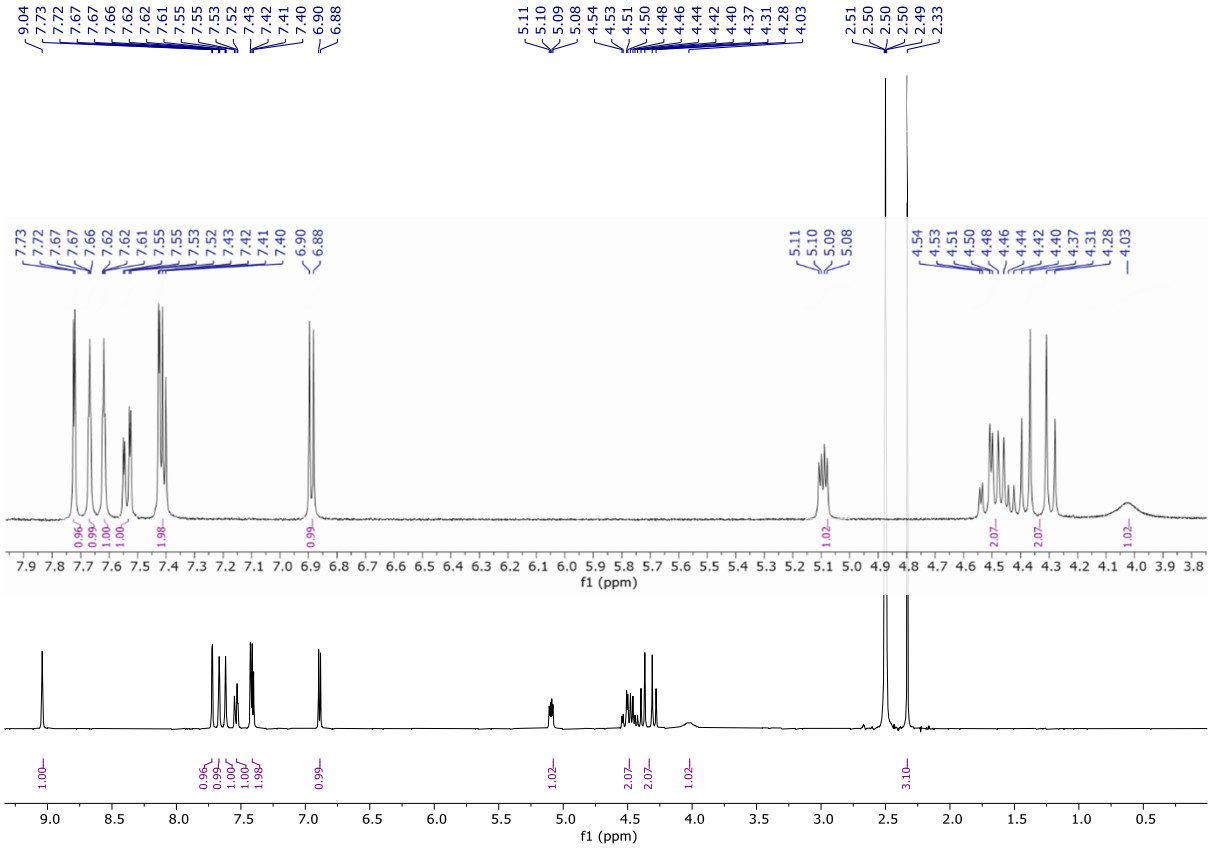


Figure S1. 400 MHz ^{1}H NMR spectrum of TCZ-Ms in DMSO-d_6 and expansion (3.7-8.0 ppm).

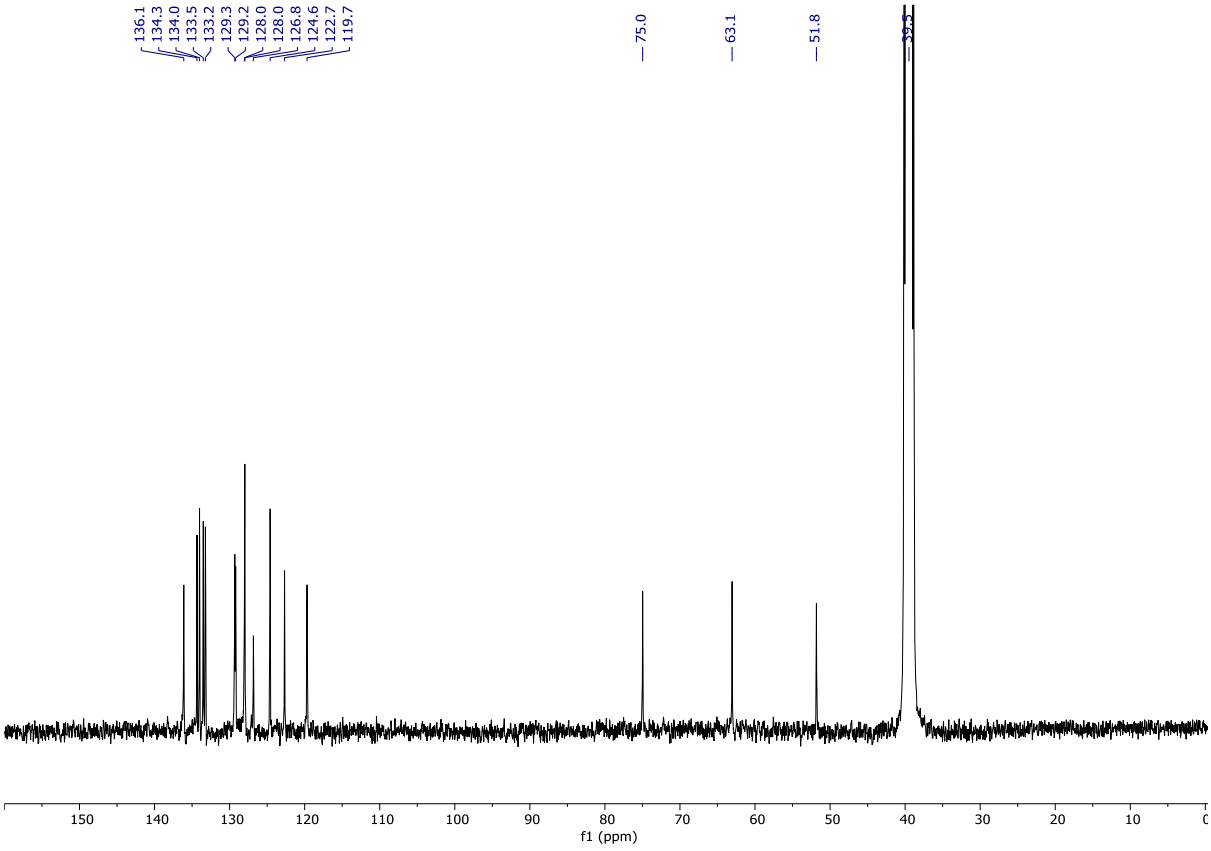


Figure S2. 100 MHz ^{13}C NMR spectrum of TCZ-Ms in DMSO-d_6.

©AUTHOR(S)

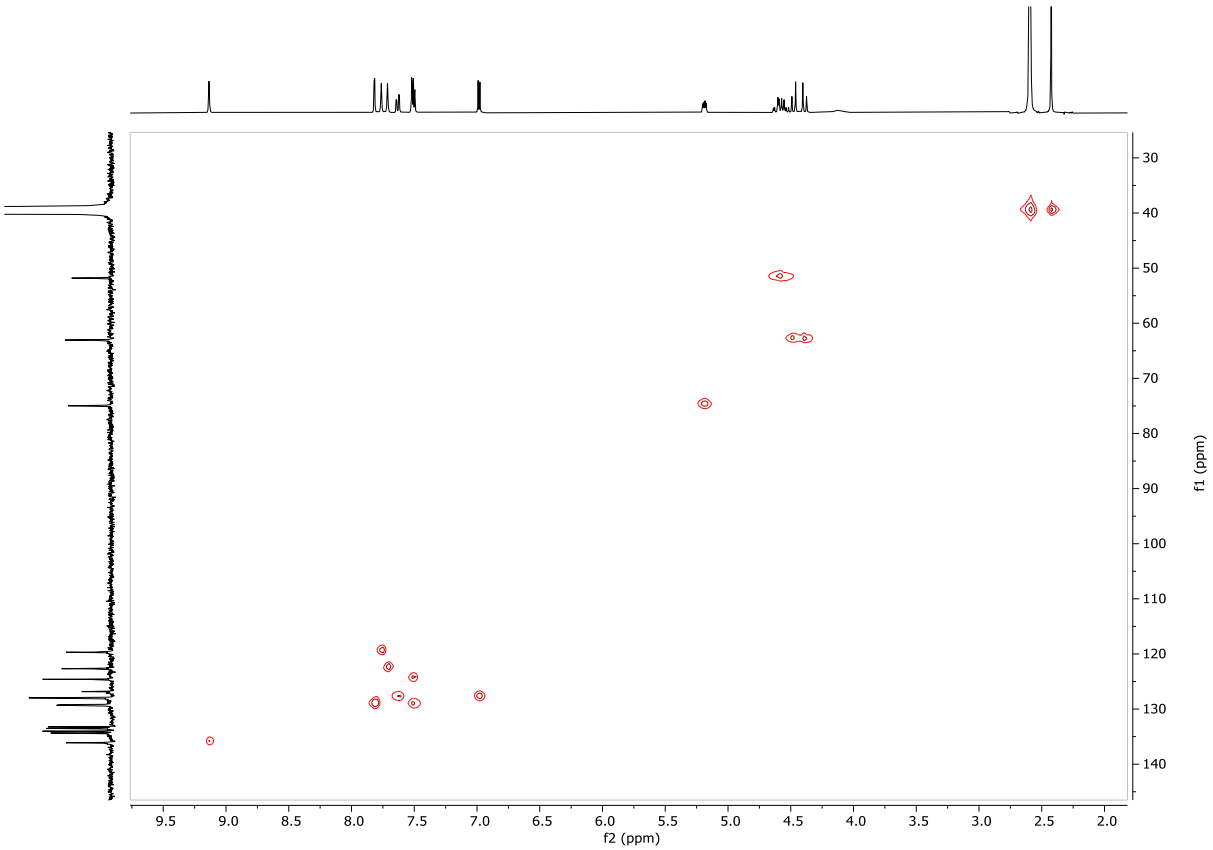


Figure S3. HSQC spectrum of TCZ-Ms in DMSO-d_6.

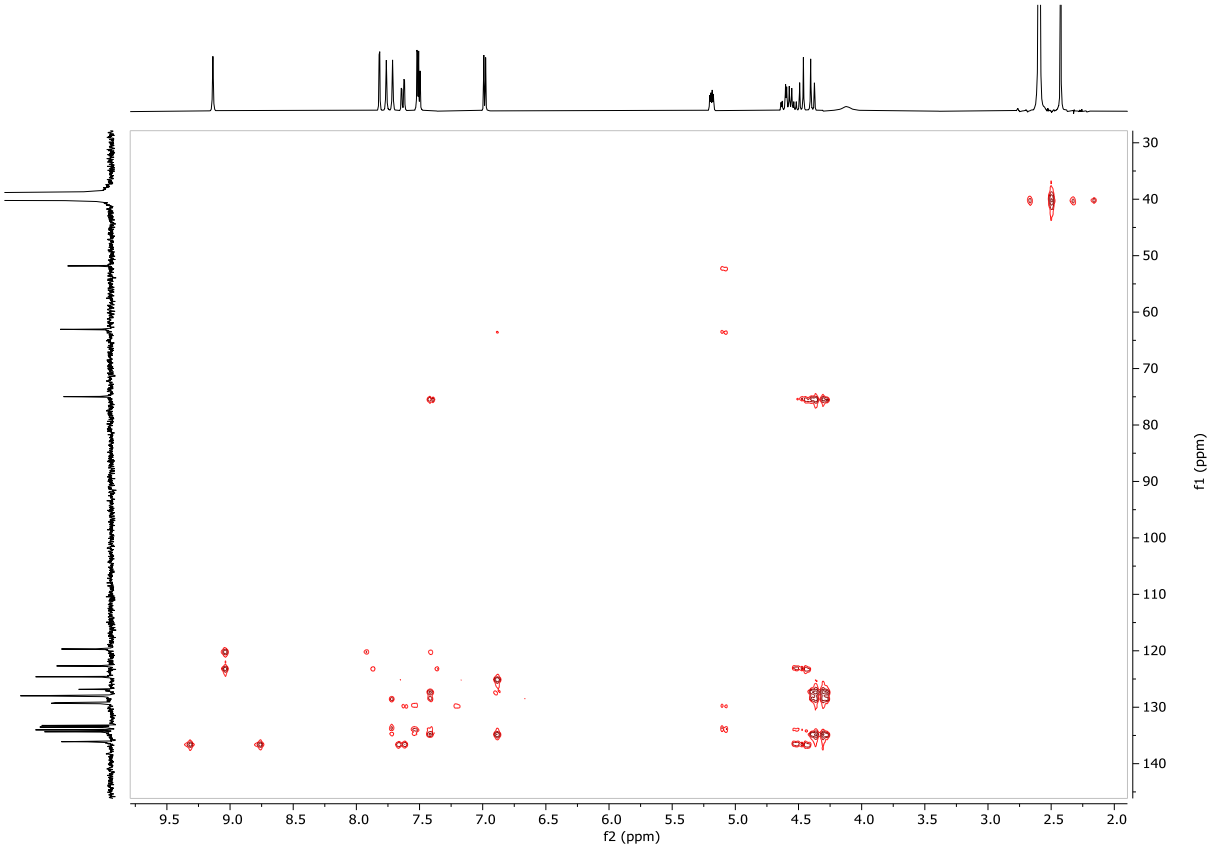


Figure S4. HMBC spectrum of TCZ-Ms in DMSO-d_6.

©AUTHOR(S)

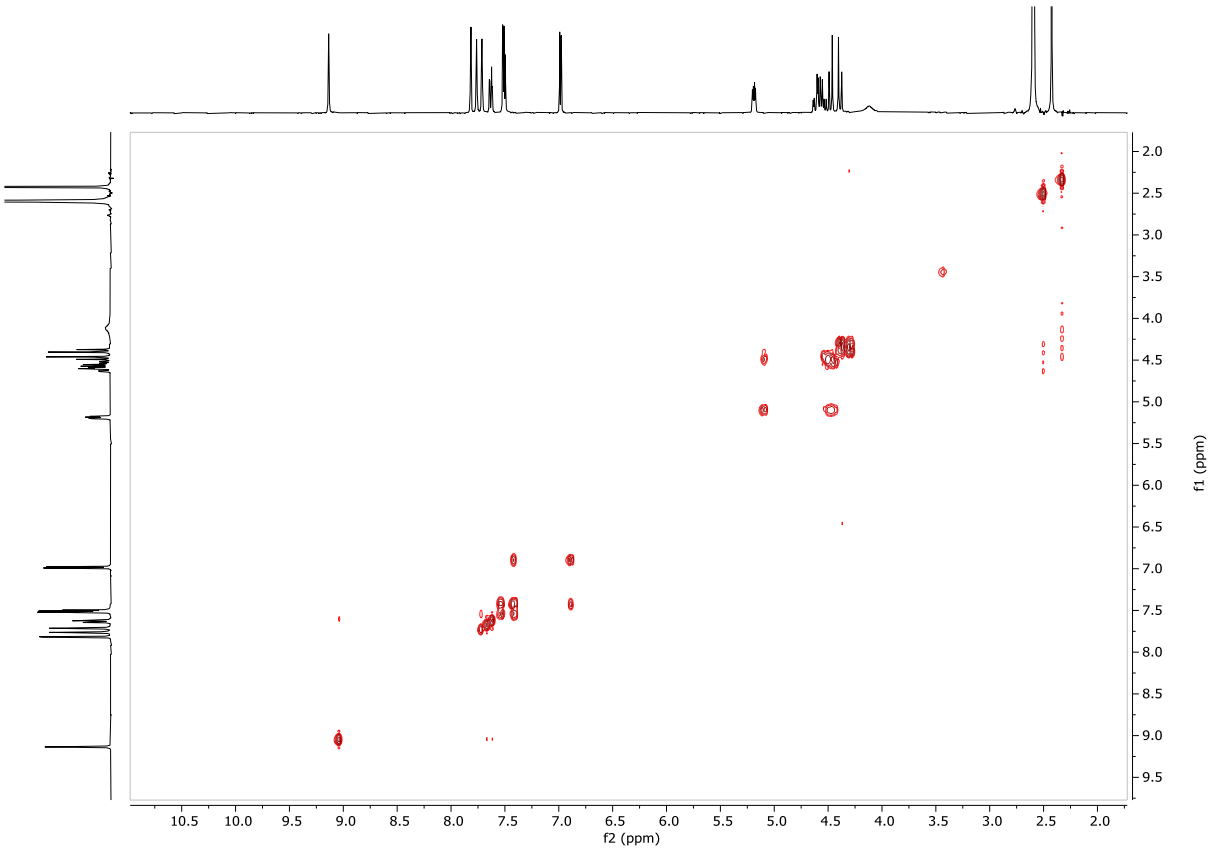


Figure S5. COSY spectrum of TCZ-Ms in DMSO-d_6.

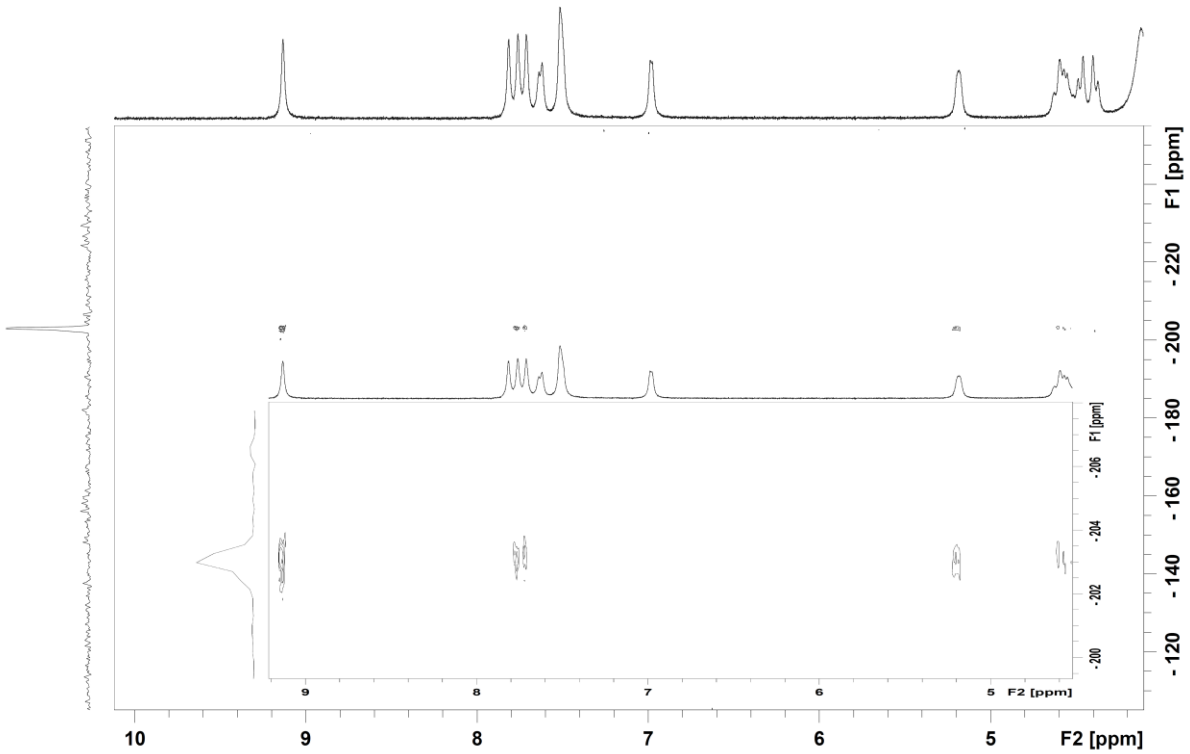


Figure S6. ^{15}N HMBC spectrum of TCZ-Ms in DMSO-d_6 and expanded view of y-axis.

©AUTHOR(S)

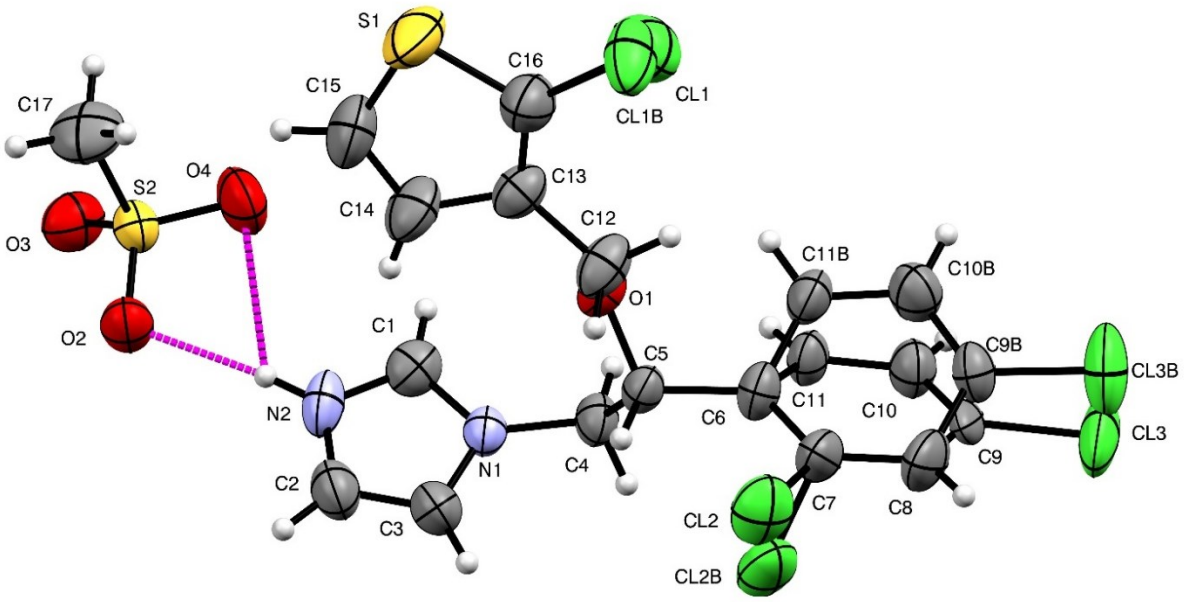


Figure S7. ORTEP representation and atom numbering of TCZ-Ms, with displacement ellipsoids drawn with a 50% probability level.

©AUTHOR(S)

Tables S1-4. Crystallographic tables of TCZ-Ms. Bond lengths, angles, torsions and H-bonds.

Table S1. Hydrogen bonds of TCZ-Ms at 289 K [Å and °]

D—H···A	*d(D—H)*	*d(H···A)*	*d(D···A)*	*<(D—H···A)*
C10[a]-H10[a]···S1[i]	0.93	2.95	3.659(8)	133.7
$C10_B$[b]-$H10_B$[b]···S1[i]	0.93	2.97	3.549(8)	121.8
C4-$H4_A$···O3[ii]	0.97	2.47	3.423(5)	168.6
C4-$H4_B$···O3[iii]	0.97	2.48	3.319(5)	144.9
C15-H15···O2[v]	0.93	2.56	3.420(5)	153.0
C1-H1···O4[ii]	0.93	2.38	3.221(5)	149.9
C2-H2···O4[vi]	0.93	2.62	3.176(5)	118.6
N2-H2N···O2	0.86	1.95	2.804(4)	173.4
N2-H2N···O4	0.86	2.61	3.180(5)	125.3
C12-$H12_B$···Cl1[a/vi]	0.97	2.84	3.810(7)	174.3
C17-$H17_B$···O2[v]	0.96	2.63	3.375(5)	134.5
C11-H11···O3[ii]	0.93	2.55	3.463(8)	165.8

Symmetry transformations used to generate equivalent atoms: (i) x, -y+2, z+1/2; (ii) -x+3/2, -y+3/2, -z+1; (iii) -x+3/2, -y+1/2, -z+1; (iv) -x+1, -y, -z+1; (v) -x+3/2, y+1/2, -z+1/2; (vi) x, y-1, z.
[a] Partition 1.

[b] Partition 2.

 ©AUTHOR(S)

Table S2. Bond distances of TCZ-Ms at 289 K [Å].

Atoms	*Distance*	*Atoms*	*Distance*
Cl2-C7	1.902(5)	C5-H5	0.9800
Cl3-C9	1.760(13)	C8-C7	1.387(5)
Cl1-C16	1.716(7)	C8-H8	0.9300
C10-C9	1.370(16)	C14-C15	1.340(5)
C10-C11	1.379(10)	C14-C13	1.454(5)
C10-H10	0.9300	C14-H14	0.9300
C11-C6	1.354(8)	C15-S1	1.678(5)
C11-H11	0.9300	C15-H15	0.9300
C9-C8	1.141(15)	O1-C12	1.421(4)
$Cl2_B$-C7	1.677(5)	N1-C1	1.335(4)
$Cl3_B$-$C9_B$	1.723(13)	C1-N2	1.317(5)
$Cl1_B$-C16	1.759(6)	C1-H1	0.9300
$C10_B$-$C9_B$	1.361(15)	C2-N2	1.348(5)
$C10_B$-$C11_B$	1.387(10)	C2-H2	0.9300
$C10_B$-$H10_B$	0.9300	N2-H2N	0.8600
$C11_B$-C6	1.496(9)	O2-S2	1.455(3)
$C11_B$-$H11_B$	0.9300	S1-C16	1.718(4)
$C9_B$-C8	1.530(13)	S2-O4	1.441(3)
C3-C2	1.335(5)	S2-C17	1.754(4)
C3-N1	1.372(5)	C6-C7	1.346(5)
C3-H3	0.9300	C12-C13	1.498(5)
O3-S2	1.435(2)	$C12-H12_A$	0.9700
C4-N1	1.467(4)	$C12-H12_B$	0.9700
C4-C5	1.514(4)	C13-C16	1.326(5)
$C4-H4_A$	0.9700	$C17-H17_A$	0.9600
$C4-H4_B$	0.9700	$C17-H17_B$	0.9600
C5-O1	1.423(4)	$C17-H17_C$	0.9600
C5-C6	1.515(4)		

©AUTHOR(S)

Table S3. Bond angles of TCZ-Ms at 289 K [°].

Angle	*Value*	*Angle*	*Value*
C9-C10-C11	118.5(9)	C7-C8-H8	119.1
C9-C10-H10	120.8	C15-C14-C13	112.1(4)
C11-C10-H10	120.8	C15-C14-H14	123.9
C6-C11-C10	121.9(6)	C13-C14-H14	123.9
C6-C11-H11	119.1	C14-C15-S1	113.4(3)
C10-C11-H11	119.1	C14-C15-H15	123.3
C8-C9-C10	120.9(11)	S1-C15-H15	123.3
C8-C9-Cl3	121.9(10)	C12-O1-C5	114.3(3)
C10-C9-Cl3	117.1(10)	C1-N1-C3	108.1(3)
$C9_B$-$C10_B$-$C11_B$	119.8(9)	C1-N1-C4	126.5(3)
$C9_B$-$C10_B$-$H10_B$	120.1	C3-N1-C4	125.3(3)
$C11_B$-$C10_B$-$H10_B$	120.1	N2-C1-N1	107.4(3)
$C10_B$-$C11_B$-C6	120.3(7)	N2-C1-H1	126.3
$C10_B$-$C11_B$-$H11_B$	119.8	N1-C1-H1	126.3
C6-$C11_B$-$H11_B$	119.8	C3-C2-N2	107.0(4)
$C10_B$-$C9_B$-C8	120.4(9)	C3-C2-H2	126.5
$C10_B$-$C9_B$-$Cl3_B$	121.6(9)	N2-C2-H2	126.5
C8-$C9_B$-$Cl3_B$	117.6(8)	C1-N2-C2	110.1(3)
C2-C3-N1	107.3(4)	C1-N2-H2N	124.9
C2-C3-H3	126.3	C2-N2-H2N	124.9
N1-C3-H3	126.3	C15-S1-C16	90.5(2)
N1-C4-C5	110.4(3)	O3-S2-O4	113.80(17)
N1-C4-$H4_A$	109.6	O3-S2-O2	112.26(16)
C5-C4-$H4_A$	109.6	O4-S2-O2	110.81(17)
N1-C4-$H4_B$	109.6	O3-S2-C17	105.8(2)
C5-C4-$H4_B$	109.6	O4-S2-C17	106.6(2)
$H4_A$-C4-$H4_B$	108.1	O2-S2-C17	107.0(2)
O1-C5-C4	106.2(2)	C7-C6-C11	110.3(4)

©AUTHOR(S)

Angle	*Value*	*Angle*	*Value*
O1-C5-C6	113.8(3)	C7-C6-C11*B*	116.5(4)
C4-C5-C6	109.9(3)	C7-C6-C5	124.2(3)
O1-C5-H5	108.9	C11-C6-C5	121.0(4)
C4-C5-H5	108.9	$C11_B$-C6-C5	116.6(4)
C6-C5-H5	108.9	C6-C7-C8	123.8(4)
C9-C8-C7	121.8(7)	C6-C7-$Cl2_B$	116.7(3)
C7-C8-$C9_B$	115.6(6)	C8-C7-$Cl2_B$	113.5(3)
C9-C8-H8	119.1	C6-C7-Cl2	115.7(3)
C8-C7-Cl2	117.5(3)	C13-C16-S1	113.9(3)
O1-C12-C13	108.6(3)	Cl1-C16-S1	122.9(3)
O1-C12-$H12_A$	110.0	C13-C16-$Cl1_B$	129.2(4)
C13-C12-$H12_A$	110.0	S1-C16-$Cl1_B$	115.6(3)
O1-C12-$H12_B$	110.0	S2-C17-$H17_A$	109.5
C13-C12-$H12_B$	110.0	S2-C17-$H17_B$	109.5
$H12_A$-C12-$H12_B$	108.4	$H17_A$-C17-$H17_B$	109.5
C16-C13-C14	110.0(3)	S2-C17-$H17_C$	109.5
C16-C13-C12	126.6(4)	$H17_A$-C17-$H17_C$	109.5
C14-C13-C12	123.3(4)	$H17_B$-C17-$H17_C$	109.5
C13-C16-Cl1	121.9(4)		

©AUTHOR(S)

Table S4. Torsion angles [°] for TCZ-Ms.

Torsion angle	*Value*	*Torsion angle*	*Value*
C(9)-C(10)-C(11)-C(6)	5.7(14)	C(4)-C(5)-C(6)-C(7)	-115.3(4)
C(11)-C(10)-C(9)-C(8)	3.2(16)	O(1)-C(5)-C(6)-C(11)	-80.3(6)
C(11)-C(10)-C(9)-Cl(3)	178.5(7)	C(4)-C(5)-C(6)-C(11)	38.7(6)
C(9B)-C(10B)-C(11B)-C(6)	-2.4(14)	O(1)-C(5)-C(6)-C(11B)	-35.2(5)
C(11B)-C(10B)-C(9B)-C(8)	-8.2(15)	C(4)-C(5)-C(6)-C(11B)	83.7(5)
C(11B)-C(10B)-C(9B)-Cl(3B)	179.6(8)	C(11)-C(6)-C(7)-C(8)	20.3(7)
N(1)-C(4)-C(5)-O(1)	-63.8(3)	C(11B)-C(6)-C(7)-C(8)	-22.4(7)
N(1)-C(4)-C(5)-C(6)	172.7(3)	C(5)-C(6)-C(7)-C(8)	176.6(4)
C(10)-C(9)-C(8)-C(7)	0.4(14)	C(11B)-C(6)-C(7)-Cl(2B)	-173.4(5)
Cl(3)-C(9)-C(8)-C(7)	-174.7(5)	C(5)-C(6)-C(7)-Cl(2B)	25.6(6)
C(10B)-C(9B)-C(8)-C(7)	4.2(12)	C(11)-C(6)-C(7)-Cl(2)	-179.9(5)
Cl(3B)-C(9B)-C(8)-C(7)	176.7(6)	C(5)-C(6)-C(7)-Cl(2)	-23.5(5)
C(13)-C(14)-C(15)-S(1)	-1.3(5)	C(9)-C(8)-C(7)-C(6)	-13.6(10)
C(4)-C(5)-O(1)-C(12)	157.5(3)	C(9B)-C(8)-C(7)-C(6)	12.1(8)
C(6)-C(5)-O(1)-C(12)	-81.5(3)	C(9B)-C(8)-C(7)-Cl(2B)	163.9(6)
C(2)-C(3)-N(1)-C(1)	-0.4(4)	C(9)-C(8)-C(7)-Cl(2)	-173.2(7)
C(2)-C(3)-N(1)-C(4)	177.6(3)	C(5)-O(1)-C(12)-C(13)	-153.6(3)
C(5)-C(4)-N(1)-C(1)	108.2(4)	C(15)-C(14)-C(13)-C(16)	1.8(5)
C(5)-C(4)-N(1)-C(3)	-69.4(4)	C(15)-C(14)-C(13)-C(12)	179.1(4)
C(3)-N(1)-C(1)-N(2)	0.3(4)	O(1)-C(12)-C(13)-C(16)	-130.1(4)
C(4)-N(1)-C(1)-N(2)	-177.7(3)	O(1)-C(12)-C(13)-C(14)	53.1(5)
N(1)-C(3)-C(2)-N(2)	0.4(4)	C(14)-C(13)-C(16)-Cl(1)	-169.3(4)
N(1)-C(1)-N(2)-C(2)	0.0(4)	C(12)-C(13)-C(16)-Cl(1)	13.5(6)
C(3)-C(2)-N(2)-C(1)	-0.2(4)	C(14)-C(13)-C(16)-S(1)	-1.6(5)
C(14)-C(15)-S(1)-C(16)	0.3(4)	C(12)-C(13)-C(16)-S(1)	-178.8(3)
C(10)-C(11)-C(6)-C(7)	-16.1(10)	C(14)-C(13)-C(16)-Cl(1B)	164.7(4)
C(10)-C(11)-C(6)-C(5)	-173.3(7)	C(12)-C(13)-C(16)-Cl(1B)	-12.4(7)
C(10B)-C(11B)-C(6)-C(7)	17.5(10)	C(15)-S(1)-C(16)-C(13)	0.8(4)
C(10B)-C(11B)-C(6)-C(5)	180.0(7)	C(15)-S(1)-C(16)-Cl(1)	168.4(4)
O(1)-C(5)-C(6)-C(7)	125.8(4)	C(15)-S(1)-C(16)-Cl(1B)	-167.5(3)

©AUTHOR(S)

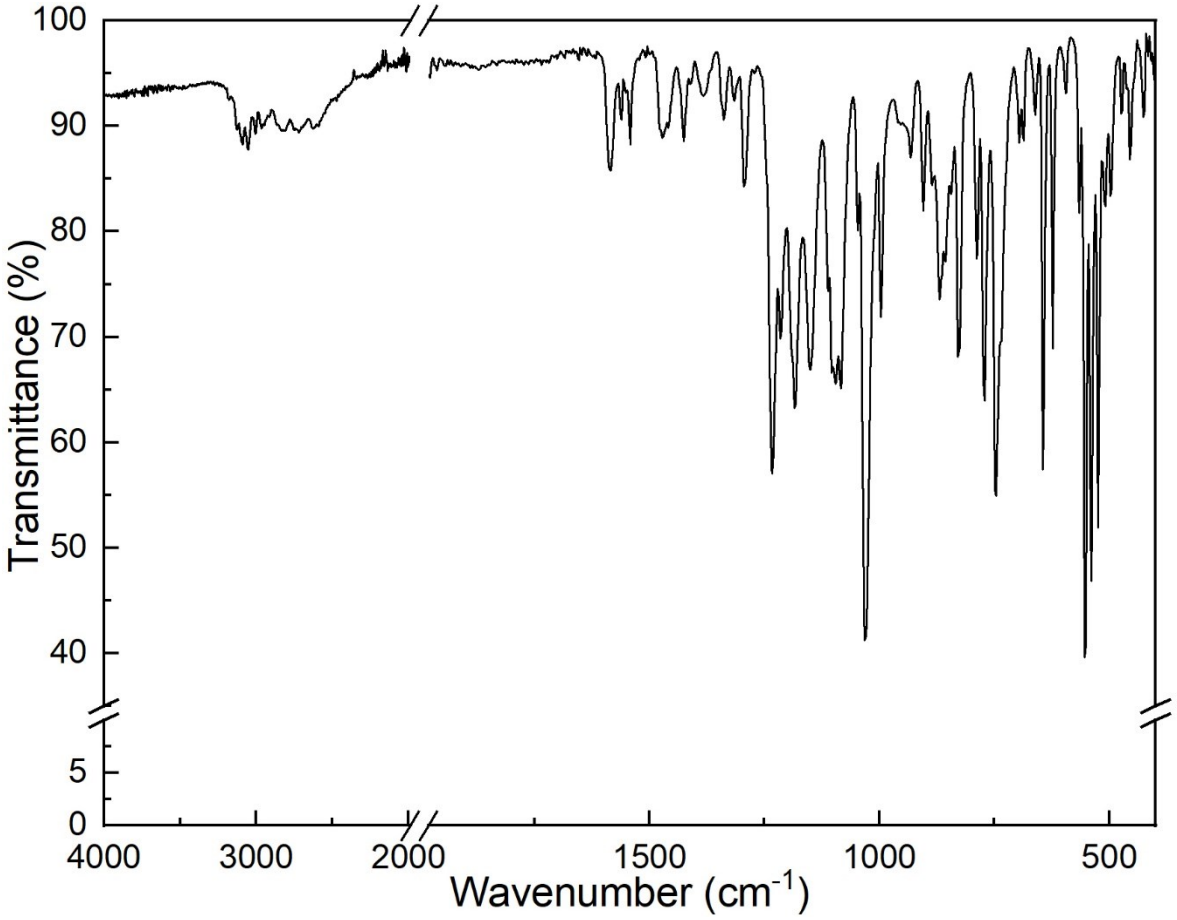


Figure S8. ATR/MIR spectrum of TCZ-Ms in the wavenumber range 400-4000 cm^{-1}.

©AUTHOR(S)

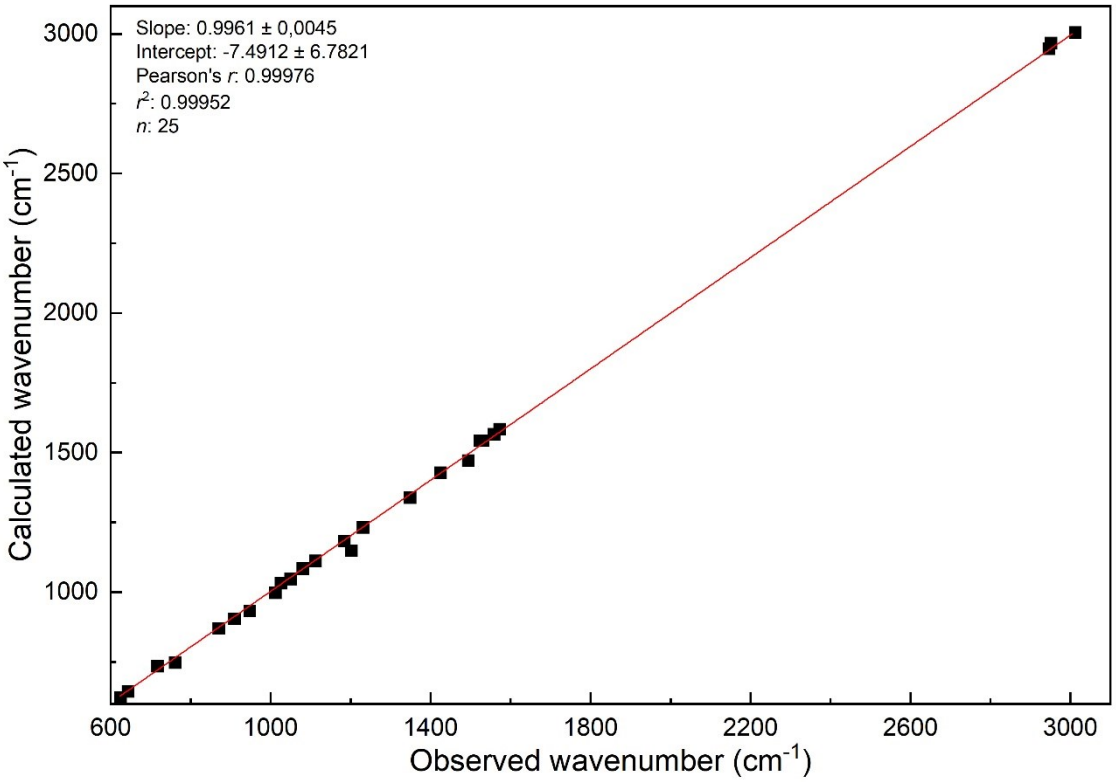


Figure S9. Correlation between observed and calculated vibrational frequencies of TCZ-Ms in the MIR region.

©AUTHOR(S)

Table S5. Experimental ATR/MIR spectra of TCZ and TCZ-Ms along with the most relevant calculated bands for TCZ-Ms and their corresponding assignments.

Wavenumber (cm^{-1})			Assignment
TCZ	TCZ-Ms	TCZ-Ms (calcd.)[a]	
735, 692, 658, 629	747, 735, 644, 623	761, 717, 643, 625	γ_{C-H}, substitution pattern of aromatic rings
993, 907	997, 870	1012, 870	δ_{C-H}, aromatic ring
1098, 1067	1047	1050	ν_{C-O}, ether
-	932, 904	948, 910	$\nu_{S-O,}$ ν_{SO3-} (symmetric, asymmetric)
1118, 1030, 1022	1084	1081	ν_{C-N}, imidazole
-	1184, 1032	1184, 1026	$\nu_{S=O}$ (asymmetric, symmetric)
1562, 1433,	1543, 1338	1524, 1349	$\nu_{C=C}$, thiophene
1589, 1467, 1388, 1281, 1184, 1137	1565, 1543, 1427, 1231, 1149, 1112	1559, 1531, 1425, 1231, 1202, 1112	$\nu_{C=C}$, phenyl
1503	1472	1494	$\nu_{C=N}$, imidazole
-	1584	1573	ν_{N-H}, imidazole
2936, 2868 2885, 2949	3005, 2967, 2947	3012, 2952, 2946	ν_{C-H}, aliphatic (asymmetric, symmetric)
-	3178		ν_{N-H}, protonated imidazole

[a]The molecular geometries were optimized to their energy minima using Gaussian09W software.[1] All calculations were performed within the framework of density functional theory (DFT), employing the B3LYP functional in combination with the 6–311++G(d,p) basis set.[2] The absence of imaginary frequencies in the computed IR spectra confirmed that the optimized structures correspond to true minima on the potential energy surface. A frequency scaling factor of 0.9613 was applied.[3]

©AUTHOR(S)

Table S6. Stability of TCZ-Ms. Main characteristics of the heating/cooling cycles.

Event	Cycle N°	1	2	4	8
Melting endotherm	T_{ons} (°C)	202.0	188.9	189.3	182.6
	T_{peak} (°C)	205.6	199.7	199.3	195.4
	T_{out} (°C)	210.0	205.5	204.4	201.8
	ΔH	-21.2	-16.4	-15.7	-12.4
	FWHM (°C)	3.6	5.8	4.9	7.3
Recrystallization exotherm	T_{ons} (°C)	119.3	113.7	116.0	109.9
	T_{peak} (°C)	113.7	108.4	109.1	102.1
	T_{out} (°C)	109.2	101.2	103.6	94.9
	ΔH	5.3	4.3	4.8	3.1
	FWHM (°C)	5.0	5.4	5.1	6.8

©AUTHOR(S)

References

1 M.J. Frisch, G.W. Trucks, H.B. Schlegel, G.E. Scuseria, M.A. Robb, J.R. Cheeseman, G. Scalmani, V. Barone, B. Mennucci, G.A. Petersson, H. Nakatsuji, M. Caricato, X. Li, H.P. Hratchian, A.F. Izmaylov, J. Bloino, G. Zheng, J.L. Sonnenberg, M. Hada, M. Ehara, K. Toyota, R. Fukuda, J. Hasegawa, M. Ishida, T. Nakajima, Y. Honda, O. Kitao, H. Nakai, T. Vreven, J.A. Montgomery Jr., J.E. Peralta, F. Ogliaro, M. Bearpark, J.J. Heyd, E. Brothers, K.N. Kudin, V.N. Staroverov, T. Keith, R. Kobayashi, J. Normand, K. Raghavachari, A. Rendell, J.C. Burant, S.S. Iyengar, J. Tomasi, M. Cossi, N. Rega, J.M. Millam, M. Klene, J.E. Knox, J.B. Cross, V. Bakken, C. Adamo, J. Jaramillo, R. Gomperts, R.E. Stratmann, O. Yazyev, A.J. Austin, R. Cammi, C. Pomelli, J.W. Ochterski, R.L. Martin, K. Morokuma, V.G. Zakrzewski, G.A. Voth, P. Salvador, J.J. Dannenberg, S. Dapprich, A.D. Daniels, O. Farkas, J.B. Foresman, J.V. Ortiz, J. Cioslowski, D.J. Fox. Gaussian 09, Revision B.01. Gaussian, Inc., Wallingford CT (2010).

2 V.S. Kumar, Y.S. Mary, K. Pradhan, D. Brahman, Y.S. Mary, R. Thomas, M.S. Roxy, C. Van Alsenoy, Synthesis, spectral properties, chemical descriptors and light harvesting studies of a new bioactive azo imidazole compound, J. Mol. Struct. 119 (2020) 127035. DOI: 10.1016/j.molstruc.2019.127035

3 J. B. Foresman, A.E. Frisch, Exploring Chemistry with Electronic Structure Methods, 3rd ed., Gaussian, Inc.: Wallingford, CT, USA, 2015.

 ©AUTHOR(S)